

Mechanism of inositol monophosphatase, the putative target of lithium therapy

(phosphatase/phosphatidylinositol/magnesium/bipolar disorder/manic depression)

SCOTT J. POLLACK*, JOHN R. ATACK*, MICHAEL R. KNOWLES*, GEORGE MCALLISTER*, C. IAN RAGAN*,
RAYMOND BAKER†, STEPHEN R. FLETCHER†, LESLIE L. IVERSEN*†, AND HOWARD B. BROUGHTON†‡

Departments of †Chemistry and *Biochemistry, Merck Sharp & Dohme Research Laboratories, Neuroscience Research Centre, Terlings Park, Eastwick Road, Harlow, Essex CM20 2QR, United Kingdom

Contributed by Leslie L. Iversen, March 14, 1994

ABSTRACT *myo*-Inositol monophosphatase (*myo*-inositol-1-phosphate phosphohydrolase, EC 3.1.3.25) is an attractive target for mechanistic investigation due to its critical role in the phosphatidylinositol signaling pathway and the possible relevance of its inhibition by Li⁺ to manic depression therapy. The x-ray crystallographic structure of human inositol monophosphatase in the presence of the inhibitory metal Gd³⁺ showed only one metal bound per active site, whereas in the presence of Mn²⁺, three ions were present with one being displaced upon phosphate binding. We report here modeling, kinetic, and mutagenesis studies on the enzyme, which reveal the requirement for two metal ions in the catalytic mechanism. Activity titration curves with Zn²⁺ or Mn²⁺ in the presence or absence of Mg²⁺ are consistent with a two-metal mechanism. Modeling studies based on the various x-ray crystallographic structures (including those with Gd³⁺ and substrate bound) further support a two-metal mechanism and define the positions of the two metal ions relative to substrate. While the first metal ion may activate water for nucleophilic attack, a second metal ion, coordinated by three aspartate residues, appears to act as a Lewis acid, stabilizing the leaving inositol oxyanion. In this model, the 6-OH group of substrate acts as a ligand for this second metal ion, consistent with the reduced catalytic activity observed with substrate analogues lacking the 6-OH. Evidence from Tb³⁺ fluorescence quenching and the two-metal kinetic titration curves suggests that Li⁺ binds at the site of this second metal ion.

In the phosphatidylinositol second-messenger pathway, receptor-activated phospholipase C hydrolyzes phosphatidylinositol 4,5-bisphosphate, to form two second messengers, inositol 1,4,5-trisphosphate and diacylglycerol, leading to Ca²⁺ and protein kinase C-mediated signal transduction, respectively (1–3). Inositol 1,4,5-trisphosphate is subsequently metabolized in a series of pathways, regenerating inositol for reincorporation into inositol phospholipids, thereby maintaining this signaling cycle. *myo*-Inositol monophosphatase (IMPase; *myo*-1-phosphate phosphohydrolase, EC 3.1.3.25) catalyzes the last hydrolytic step in these pathways, regenerating *myo*-D-inositol from *myo*-D-inositol 1-phosphate [Ins(1)P], Ins(3)P, or Ins(4)P (4).

IMPase, a homodimer of two 30-kDa subunits, requires Mg²⁺ for activity, though Mn²⁺ and Zn²⁺ support catalysis to different extents (*vide infra*). Magnesium may act to stabilize the transition-state geometry, activate water or a protein nucleophile, stabilize the leaving inositol oxyanion, or through some combination of these mechanisms.

Inhibition of IMPase by Li⁺ and the resulting effects on phosphatidylinositol signaling responses may account for the

effects of Li⁺ in manic depression therapy (5–7). Inhibition by Li⁺ is uncompetitive with respect to substrate (4, 5), and therefore Li⁺ exerts its greatest effect at high substrate concentrations (8), possibly explaining the selectivity of Li⁺ for cells with excessive phosphatidylinositol signal-transduction activity (6).

X-ray crystallographic reports on human IMPase described the active site in the presence of Gd³⁺ and sulfate (9) and, more recently, in the presence of Gd³⁺ and Ins(1)P or Ins(3)P (10). However, these structures could be misleading because Gd³⁺ is a large, trivalent metal, typically with two to three more ligands than Mg²⁺ and, hence, may not bind at the same site(s). Gd³⁺ may also occupy only one metal-binding site due to competition by Li⁺ for other possible sites because high Li⁺ concentrations were present in the crystallography conditions (9, 10) and bound Li⁺ would not have been crystallographically detectable.

Recently, the structure of human IMPase was solved to 2.6-Å resolution in the presence of Mn²⁺ ions and no other metal (11). This structure revealed three Mn²⁺ ions bound per active site, one of which could be displaced by soaking inorganic phosphate, a competitive inhibitor of IMPase, into the crystal. Because substrate was absent from the manganese structures, these findings left open to speculation whether the second and, possibly, third metal ions are required for catalysis, are inhibitory, or are artifacts. We report here findings that reveal the requirement for two Mg²⁺ ions in the catalytic mechanism and discuss their implications on the nature of Li⁺ inhibition.

MATERIALS AND METHODS

Modeling Studies. Sybyl software (Tripos Associates, St. Louis) was used with the Kollman united-atom force field (12). Parameters for Gd³⁺, Mn²⁺, and Li⁺ were added from the metals parameter set distributed by Tripos. The Mn²⁺ and Li⁺ parameters gave contacts in agreement with those seen in the Cambridge Crystallographic Database (13), but to achieve similarly satisfactory results the van der Waals radius parameter of Gd³⁺ was reduced to 2.1 Å. Hydrogens were added to the protein by using the Sybyl BIOPOLY ADDH command. The standard Sybyl TIP3P water model was used for crystallographically observed water molecules. Charges were taken from the standard Kollman parameter set for water molecules and protein residues. Starting coordinates for dianionic Ins(1)P were obtained from the crystal structure of the IMPase/Gd/Ins(1)P complex, supplemented with hydrogens at idealized sites on the inositol moiety, and opti-

Abbreviations: IMPase, *myo*-inositol monophosphatase; Ins(1)P, D-*myo*-inositol 1-phosphate; E70Q, the human IMPase mutant in which Glu-70 (indicated by its standard single-letter abbreviation) was converted to Gln, other mutations being indicated similarly. ‡To whom reprint requests should be addressed.

The publication costs of this article were defrayed in part by page charge payment. This article must therefore be hereby marked "advertisement" in accordance with 18 U.S.C. §1734 solely to indicate this fact.

mized for geometry; charges were assigned by using MOPAC 6 [QCPE (Indiana University, Bloomington) program 455; ref. 14] with the keywords AM1 PRECISE ESP CHARGE=-2.

Environments of metal atoms and the ligand Ins(1)*P* were analyzed in terms of "definite contact," "possible contact," and "no contact" on the basis of the following distance criteria from heteroatom to metal or proton:

	Definite contact	Possible contact	No contact
Gd ³⁺	<3.5 Å	3.5–3.8 Å	>3.8 Å
Li ⁺	<2.7 Å	2.7–3.0 Å	>3.0 Å
Mn ²⁺	<3.4 Å	3.4–3.7 Å	>3.7 Å
H ⁺ (prerefinement)	<2.0 Å	2.0–3.0 Å	>3.0 Å
H ⁺ (postrefinement)	<2.0 Å	2.0–2.2 Å	>2.2 Å

Chemicals. DL-Ins(1)*P* was prepared by the method of Billington *et al.* (15), and L-[U-¹⁴C]Ins(1)*P* was obtained from Amersham. All other chemicals were obtained from commercial suppliers.

Mutagenesis and Enzyme Assays. Oligonucleotide-directed mutagenesis was done by the method of Kunkel *et al.* (16) as described (17). Purification and quantification of wild-type and mutant human IMPase expressed in *Escherichia coli* were done as described (18). IMPase activity was measured by a described radiochemical assay (19), in which ¹⁴C-labeled inositol produced from ¹⁴C-labeled Ins(1)*P* [0.21 Ci/mol (1 Ci = 37 GBq); initial concentration, 100 μM] is separated from the unhydrolyzed substrate by anion-exchange chromatography over Dowex-formate columns. The buffer was 50 mM Tris·HCl, pH 7.8/250 mM KCl/3 mM MgCl₂, except in Mg²⁺, Mn²⁺, and Zn²⁺ titrations, where the metal ion concentration was varied and KCl was omitted. Tb³⁺ fluorescence quenching experiments were done exactly as described (17).

RESULTS AND DISCUSSION

Magnesium Dependence of IMPase. At relatively low concentrations (<5 mM), Mg²⁺ acts as a noncompetitive activator with respect to substrate (5, 20), whereas at higher concentrations (>5 mM), Mg²⁺, like Li⁺, becomes an uncompetitive inhibitor (21, 22). Previous kinetic (21, 22) and mutagenesis (17) studies have shown that Li⁺ and Mg²⁺ inhibitory bindings are mutually exclusive and occur at a similar site. This mode of inhibition together with direct kinetic evidence from previous Mg²⁺ dependence studies (22) called for an ordered mechanism in which Mg²⁺ binds after substrate.

However, the two different modes of Mg²⁺ behavior (noncompetitive activation and uncompetitive inhibition) suggest two different mechanisms of binding. Furthermore, the direct measurement of Mg²⁺ binding to IMPase by Tb³⁺ fluorescence quenching (17) did not require the presence of substrate. In contrast, phosphate (a competitive inhibitor with respect to substrate) was seen to bind *only* when Mg²⁺ was present (23). Together these results suggest that Mg²⁺ binding must precede *and* follow substrate binding. A two-metal mechanism could reconcile these findings. Previous observations that Mg²⁺ binding is cooperative (Hill coefficient = 2.0) (21, 22) and that this cooperativity is substrate dependent (22) were originally rationalized by invoking interactions between the two subunits of the homodimer (21, 22). However, the two active sites are >30 Å apart, and these effects are more likely related to two metal ions in each active site.

Two-Metal Titrations. In the absence of Mg²⁺, IMPase was active in the presence of Zn²⁺ or Mn²⁺, with optimal specific activities of ≈50% and 25%, respectively, that with Mg²⁺.

For both Zn²⁺ and Mn²⁺, optimal activity occurred at 300 μM ($K_m = 50 \mu\text{M}$). As with Mg²⁺, inhibition occurred at higher concentrations (IC₅₀ = 2 mM for both metals). In the presence of Mg²⁺, low concentrations of Zn²⁺ (or Mn²⁺) inhibited the Mg²⁺-activated enzyme, whereas higher concentrations of Zn²⁺ (or Mn²⁺) became activating again (Fig. 1).

These results indicate that at least two metal ions in kinetically distinct environments are required for enzyme activity. As the concentration of Zn²⁺ (or Mn²⁺) increases, the observed effect on the catalytic rate corresponds to the conversion of a (Mg²⁺, Mg²⁺)-containing species to a (Zn²⁺, Mg²⁺) species and finally a (Zn²⁺, Zn²⁺) species. Although Zn²⁺ (or Mn²⁺) binding at the first site appeared competitive with respect to Mg²⁺ (IC₅₀ increases at higher Mg²⁺ concentrations; Fig. 1), binding at the second site was noncompetitive with respect to Mg²⁺, with activation occurring at the same concentration ($K_m = 50 \mu\text{M}$) of Zn²⁺ (or Mn²⁺) when a range of Mg²⁺ concentrations (including no Mg²⁺) was used. The pattern of a final inhibitory phase at high Zn²⁺ or Mn²⁺ concentrations, also found in Mg²⁺-dependence curves, fits a model in which metal remaining bound after the catalytic step becomes inhibitory (17, 22). Given the apparent K_m values for Zn²⁺, Mn²⁺ (both 50 μM), and Mg²⁺ (150 μM) and the low (submicromolar) *in vivo* concentrations of Zn²⁺ and Mn²⁺ vs. that of Mg²⁺ (≈1 mM), the Mg²⁺-activated enzyme should be most relevant to physiological catalysis.

Crystallographic studies have shown one (Ca²⁺ and Gd³⁺/Li⁺ forms), two, or three (Mn²⁺ form in the presence and absence of phosphate, respectively) metal ions in the active site of IMPase (9–11), making it unclear how many metal ions are involved in catalysis. Recent binding studies on bovine IMPase measuring ⁴⁵Ca²⁺ displacement by Mg²⁺ indicate that there are two high-affinity (100 μM < K_d < 300 μM) and one low-affinity ($K_d > 1 \text{ mM}$) Mg²⁺ sites in this enzyme (P. Greasley and M. Gore, personal communication). This finding is consistent with the structural report and suggests that a low-affinity Mg²⁺ (or Mn²⁺) site may be present under some conditions but would be readily displaced during catalysis. The likelihood that IMPase operates *via* a two-metal mechanism is strengthened by the finding that fructose-1,6-bisphosphatase (D-fructose-1,6-bisphosphate 1-phosphohydrolase, EC 3.1.3.11), another Li⁺-sensitive enzyme with strong local sequence homology to IMPase in the metal-binding region (in addition to a similar overall secondary-structure topology) uses a two-metal (Mn²⁺ or Zn²⁺) mechanism (24, 25).

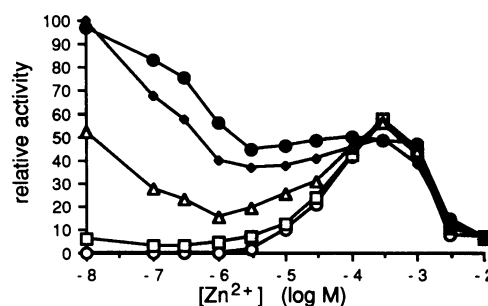


FIG. 1. Activity of human IMPase as a function of [Zn²⁺] at different Mg²⁺ concentrations: no Mg²⁺ (○), 0.1 mM (□), 0.3 mM (△), 1 mM (◇), and 3 mM (●) Mg²⁺. In the initial inhibitory phase, IC₅₀ for Zn²⁺ increased at higher [Mg²⁺], indicating competitive Zn²⁺ binding with respect to Mg²⁺. For example, IC₅₀ was 0.2 μM at 0.3 mM Mg²⁺ and 0.5 μM at 1 mM Mg²⁺. At higher Zn²⁺ concentrations, the activating and inhibitory phases observed occurred at the same concentration ranges ($K_m = 50 \mu\text{M}$; IC₅₀ = 2 mM) at various Mg²⁺ concentrations, indicating noncompetitive binding with respect to Mg²⁺ in this range of [Zn²⁺]. Mn²⁺ titration curves were similar but with lower levels of activation than seen with Zn²⁺ (data not shown).

Modeling Studies. To predict the "metallation" state of catalytically active IMPase and to view its experimentally inaccessible structure in the presence of substrate, models were generated by merging x-ray crystallographic data derived from two forms of the enzyme: the inactive form in the presence of Gd^{3+} and Li^+ ions and Ins(1)*P* (10) and the active form in the presence of Mn^{2+} but no substrate (11). After superimposition of the two x-ray structures on the C_α coordinates, one of the three metal sites in the Mn^{2+} form corresponded very closely to that occupied by Gd^{3+} in the enzyme/ Gd /Ins(1)*P* complex (site 1). The other two manganese sites (site 2, liganded by the side chains of Asp-90, Asp-93, and Asp-220 and site 3, liganded only by the side chain of Glu-70) defined the remaining metal positions for the models (Fig. 2). Four models were generated containing metals at the various sites as follows:

Model	Site 1	Site 2	Site 3
Gd/Li	Gd^{3+}	Li^+	
Gd/2Li	Gd^{3+}	Li^+	Li^+
2Mn	Mn^{2+}	Mn^{2+}	
3Mn	Mn^{2+}	Mn^{2+}	Mn^{2+}

Li^+ was included in the Gd^{3+} -containing models because high concentrations of Li^+ were present in the crystallization (≈ 2 M), and kinetic and mutagenesis studies suggest that the Li^+ -binding site corresponds to one of the activating Mg^{2+} -binding sites (17, 21, 22). The water structure for the models was taken directly from that observed in the enzyme/ Gd /Ins(1)*P* complex, which was more complete than in the enzyme/ Mn structures.

Each model was annealed by partial minimization, initially only of the water molecules and then of the entire system, followed by a short (11 ps) run of molecular dynamics. The short dynamics run was used to remove excessive strain and to provide a number of sample conformations (three per model) to assess the robustness of observed interactions. Each of these sample conformations was energy-minimized to a point where an exhaustive minimization study on one model (Gd/Li) suggested there would be little change in geometry on further minimization. A short dynamics run in the absence of additional solvent and a standard (8 Å) electrostatic cut-off distance were used because the behavior of a relatively small part of a large system was being examined (26).

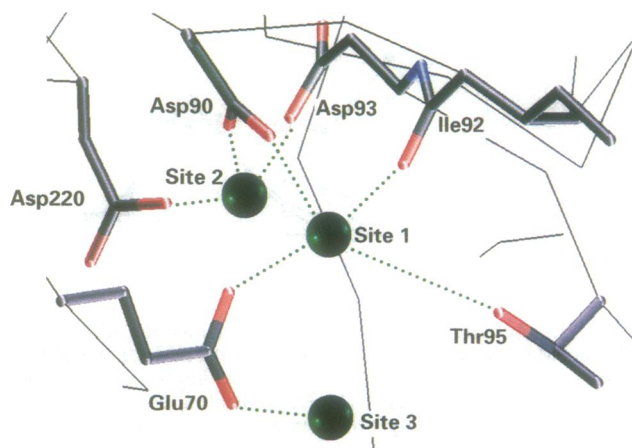


FIG. 2. The active site of human IMPase, showing positions of the three metals (green circles) seen in the Mn^{2+} structure (11) and their corresponding ligands. Colors represent atom types (red = O, blue = N, black = C).

The annealing scheme produced a number of gross changes in the structure—particularly, a hinge bend between the two subunits (Fig. 3). These large changes preclude the use of precise displacement, distance, and angle criteria to describe the effect of annealing and to analyze the environments of mechanistically significant parts of the system. However, analysis of the *local* environment of metal ions and ligand atoms was possible by the use of the definite/possible/no contact scheme outlined above.

An examination of the models derived from the 9-, 10-, and 11-ps time-point samples showed that the 2Mn model was the most consistent, both internally (across time points and at both active sites) and with known structure-activity relationships of substrates and inhibitors of IMPase. In particular, this was the only model in which the 6-OH group of Ins(1)*P* was involved consistently in a contact to the site-2 metal atom (Fig. 4A). It has been shown that substrate analogues that lack this OH group are not hydrolyzed but still bind to the enzyme (27, 28). Conversely, the 3Mn model was the only one in which the phosphate ester oxygen was not in contact with the site-2 metal (Fig. 4B), which would therefore be unable to stabilize the inositol oxyanion as a leaving group in this model, an attractive mechanistic possibility allowed by all other models (*vide infra*).

Interestingly, orientation of the inositol ring with respect to protein is the same in the 2Mn and Gd/2Li models and quite distinct from that in the 3Mn and Gd/Li models. The interactions observed in the crystal structure (10) are generally preserved in the models, although in the Mn-containing models, interactions of the 2-OH group of Ins(1)*P* are less consistent. The established importance of the 2-OH in binding (28) may be due to intermittent contact with Asp-93 (10, 17), to interactions *via* the water network, or to dipole interactions with the helix from residues 195 to 205. Alternatively, the contact with the Ala-196 backbone NH (seen in the crystal structure and preserved in the Gd/Li models) may be intermittent in the Mn models due to their simplified nature.

The Catalytic Mechanism. Phosphatase mechanisms often proceed through covalent phosphoenzyme intermediates resulting from nucleophilic attack by an active-site amino acid side chain (29). With IMPase, all attempts to trap a phosphoenzyme species or to replace the phosphoryl acceptor by other nucleophiles have failed (22, 30). Moreover, the exchange of ^{18}O from ^{18}O - H_2O into phosphate occurs only in the presence of inositol (22, 31), making a phosphoenzyme species unlikely in the absence of a protein conformational change upon inositol binding (10, 22). Finally, the crystal structures of IMPase in the presence of substrate reveal the

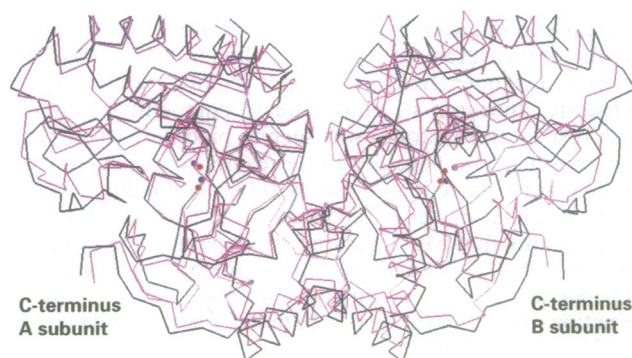


FIG. 3. Effects of energy minimization on the conformation of the enzyme; preannealed structure (magenta, metals in red) superimposed on the annealed 2Mn model (black, metals in blue) on the C_α coordinates of one subunit.

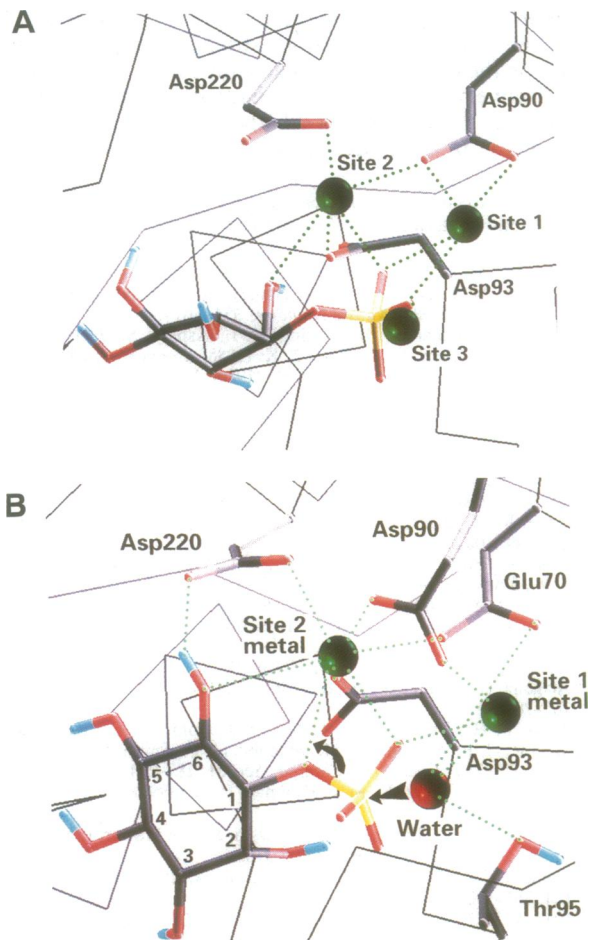


FIG. 4. The active-site structures resulting from energy minimizations on the 3Mn model (A) and the 2Mn model (B). Note the occurrence of interactions of the metal coordinated by Asp-90, Asp-93, and Asp-220 with both the 6-OH group and the bridging oxygen of inositol in the two-metal model but not in the three-metal model. Also depicted is the predicted mechanism of inositol monophosphatase, with nucleophilic attack by a Glu-70- (and possibly metal ion- and Thr-95-) activated water molecule on the phosphoryl group of Ins(1)P. A second metal ion, coordinated by Asp-90, Asp-93, and Asp-220, acts as a Lewis acid, assisting the departure of the inositol oxyanion.

lack of potentially nucleophilic side chains in the vicinity of the phosphoryl group (10).

An alternative candidate mechanism for IMPase is the direct hydrolysis of the phosphate ester by water, in which Mg^{2+} may be involved in activating water for nucleophilic attack, in substrate binding, and/or in the Lewis acid stabilization of the inositol oxyanion leaving group. These possible roles for Mg^{2+} have precedent in both enzymes (32–37) and small-molecule model systems (38, 39). Catalysis by fructose 1,6-bisphosphatase is thought to proceed through nucleophilic attack by water (24, 25), suggesting that IMPase may follow a similar direct hydrolysis mechanism.

The IMPase mutants E70Q, E70D, D90N, D93N (17), D220G (0.01% of wild-type k_{cat} ; no substantial change in K_m), and D220N (no detectable activity) all affect primarily k_{cat} . Together with the structural data, these findings support roles for all four carboxylates in the IMPase mechanism.

Overall, the structural and mutagenesis evidence is consistent with a mechanism in which a water molecule is activated for nucleophilic attack at phosphorus by a combination of Glu-70, one metal ion, and possibly Thr-95. Such a mechanism fits the 2Mn model study in which a water molecule makes close approaches during molecular dynam-

ics (a further 10-ps run starting from the 11-ps time point annealed structure) simultaneously to the site-1 Mn^{2+} (A chain distance = 3.36 Å), the substrate phosphorus (3.27 Å), and a side-chain oxygen of Glu-70 (2.89 Å) and in which the angle between the water oxygen, the phosphorus atom, and the leaving inositol oxygen is obtuse (141°) (Fig. 4B). It may also be seen that for much of the dynamics time (including the time point shown in Fig. 4B) the potential nucleophile is close (mean = 3.2 Å, SD = 0.35 Å) to the Thr-95 side-chain oxygen. This proximity is also consistent with the effect of Thr-95 mutations (17).

The effects of mutations at Asp-90, Asp-93, and Asp-220, together with the Mn^{2+} structures and modeling results, confirm that these residues coordinate a second metal ion, which may, in turn, be positioned to activate the inositol ester oxygen for departure by acting as a Lewis acid (Fig. 4B). The deleterious effect of deleting the 6-OH group of Ins(1)P (which may also coordinate this Mg^{2+}) on the catalytic rate (27, 28) is also consistent with this model. Preliminary crystallographic studies in the presence of the substrate analogue inhibitor D-3,5,6-deshydroxyinositol 1-phosphate show that the binding mode is essentially identical to that of substrate (R. Bone, L. Frank, J. P. Springer, J.R.A., unpublished data). Deletion of these OH groups may thus be interpreted in the context of the same relative ligand–protein orientation.

Nature of Inhibition by Li^+ . The uncompetitive mode of inhibition by Li^+ (and high concentrations of Mg^{2+}) implies that the metals interact with an enzyme–substrate (or –intermediate or –product) complex. Detailed kinetic analysis has suggested that Li^+ binds to a phosphate-bound enzyme species after hydrolysis (22, 30). Ganzhorn and Chanal (21) proposed a model with two Mg^{2+} sites, one activating and one inhibitory, with Li^+ occupying the latter site. From our studies it is apparent that, at least at low Mg^{2+} concentrations, both sites are activating. Upon hydrolysis and inositol departure, Mg^{2+} still bound to the enzyme–phosphate complex may inhibit the enzyme. The conformation of the metal-binding site may change slightly, allowing Li^+ to bind with greater affinity than Mg^{2+} . Another phosphate oxygen (derived from water) is available for metal binding, and Li^+

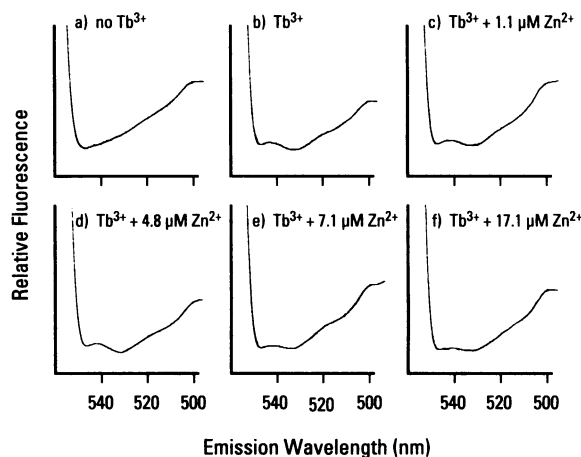


FIG. 5. Tb^{3+} fluorescence quenching by Zn^{2+} to titrate binding. The first two spectra show the fluorescence of 1.7 μM IMPase in the absence (a) and presence (b) of 35 μM $TbCl_3$. At an excitation wavelength of 295 nm, the peak at 544 nm is due to fluorescence of bound Tb^{3+} . As Zn^{2+} is added (spectra c–f), the reduction in area under this peak is used to determine IC_{50} . Half-maximal binding occurred between d and e, corresponding to an IC_{50} of $6 \pm 1 \mu M$. At 35 μM Tb^{3+} , this corresponds to a K_d of 0.16 μM (17). The experiment was also done at 70 μM $TbCl_3$, at which a K_d of 0.18 μM was seen (data not shown). The average of these values (0.17 μM) is compared with the kinetic results in *Results and Discussion*.

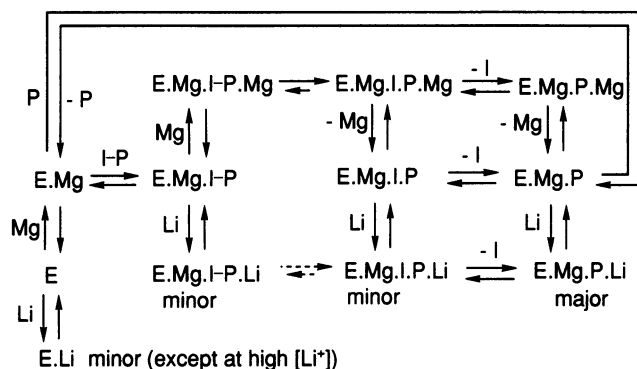


FIG. 6. Proposed kinetic scheme for IMPase catalysis and inhibition by Li⁺ or Mg²⁺. The scheme is based on this work and two previous reports (17, 22). Upon the ordered binding of the site-1 Mg²⁺, Ins(1)P (shown as I-P), and the site-2 Mg²⁺ to the enzyme (E), the catalytic reaction (top) involves the direct hydrolysis of enzyme-bound Ins(1)P in this complex (E.Mg.I-P.Mg) by water (water is not shown for clarity) followed by inositol (I) and site-2 magnesium de-binding. Inhibition by Li⁺ (or Mg²⁺) is primarily due to binding the enzyme-phosphate species (E.Mg.P) after hydrolysis and inositol departure, retarding phosphate (P) release, though other Li⁺-bound species exist. Enzyme-catalyzed hydrolysis in the presence of Li⁺ (dashed arrows) may proceed too slowly to contribute substantially to the kinetic scheme.

may form a tight complex because its size and charge are optimal for phosphate and protein coordination in the modified metal site.

Which of the two metal ion sites is occupied by Li⁺ in uncompetitive inhibition (with respect to substrate)? The results of the mutagenesis studies are ambiguous because apparent binding by both metals was affected whenever one was altered (17), consistent with the close proximity (3.8 Å) of the two sites. The Li⁺-binding site appears from the results reported here to correspond to metal site 2 (Fig. 4B). This conclusion is based on the following indirect evidence: Zn²⁺ quenches Tb³⁺-IMPase fluorescence (17) with high affinity ($K_d = 0.17 \pm 0.01 \mu\text{M}$) (Fig. 5). Because Tb³⁺ and Gd³⁺ are of similar size, this finding suggests that the inhibitory Zn²⁺ [the "first" or higher-affinity site in the Zn²⁺ titration curves, Fig. 1 (apparent $K_i = 0.10 \pm 0.02 \mu\text{M}$)] binds at the heavy metal site seen in the Gd³⁺ structure (site 1) (9, 10). This inhibitory binding by Zn²⁺ is competitive with respect to Mg²⁺. At the "second" or lower-affinity Zn²⁺ site, activation ($K_m = 50 \mu\text{M}$) and finally inhibition ($\text{IC}_{50} = 2 \text{ mM}$) was noncompetitive with respect to Mg²⁺, as is Li⁺ inhibition (21, 22).

The kinetic mechanism of IMPase and of its inhibition by Li⁺ is summarized in Fig. 6. This scheme is modified from two reports (17, 22) in view of the requirement for a two-metal mechanism. Note that the first Mg²⁺ remains bound throughout the catalytic cycle, whereas the second ion comes on and off during catalysis, becoming inhibitory if remaining bound. Li⁺ binds primarily to the phosphate-bound form of the enzyme after hydrolysis occurs but can also bind other forms of the enzyme, including the free enzyme (17, 22).

Although this study contributes to our understanding of the structure and mechanism of IMPase, we have not conclusively demonstrated how Li⁺ inhibits the enzyme. It has been difficult to obtain structural information about Li⁺ binding at the available x-ray crystallographic resolution. Although the mode of Li⁺ binding to IMPase is of intense interest from the

viewpoint of understanding the molecular basis for Li⁺ treatment of manic depression, structural and mechanistic studies on the enzyme are perhaps more important for future drug-discovery efforts. The search for an alternative inhibitor may answer the question of whether IMPase is, indeed, the target of Li⁺ in manic depression therapy.

We thank Rosamond G. Jackson for her early experimental work on the kinetic behavior of IMPase in the presence of Mg²⁺ and Zn²⁺.

- Berridge, M. J. & Irvine, R. F. (1989) *Nature (London)* **341**, 197-205.
- Berridge, M. J., Downes, C. P. & Hanley, M. R. (1989) *Cell* **59**, 411-419.
- Nishizuka, Y. (1988) *Nature (London)* **334**, 661-665.
- Gee, N. S., Ragan, C. I., Watling, K. I., Aspley, S., Jackson, R. G., Reid, G. R., Gani, D. & Shute, J. K. (1988) *Biochem. J.* **249**, 883-889.
- Hallcher, L. M. & Sherman, W. R. (1980) *J. Biol. Chem.* **255**, 10896-10901.
- Nahorski, S. R., Ragan, C. I. & Challiss, R. A. J. (1991) *Trends Pharmacol. Sci.* **12**, 297-303.
- Nahorski, S. R., Jenkinson, S. & Challiss, R. A. J. (1992) *Biochem. Soc. Trans.* **20**, 430-434.
- Cornish-Bowden, A. (1986) *FEBS Lett.* **203**, 3-6.
- Bone, R., Springer, J. P. & Atack, J. R. (1992) *Proc. Natl. Acad. Sci. USA* **89**, 10031-10035.
- Bone, R., Frank, L., Springer, J. P., Pollack, S. J., Osborne, S., Atack, J. R., Knowles, M. R., McAllister, G., Ragan, C. I., Broughton, H. B., Baker, R. & Fletcher, S. R. (1994) *Biochemistry*, in press.
- Bone, R., Frank, L., Springer, J. P. & Atack, J. R. (1994) *Biochemistry*, in press.
- Kollman, P. A., Weiner, S. J., Case, D. A., Singh, U. C., Ghio, C., Alagona, G., Profeta, S., Jr., & Weiner, P. (1984) *J. Am. Chem. Soc.* **106**, 765-784.
- Allen, F. H., Davies, J. E., Galloy, J. J., Johnson, O., Kennard, O., Macrae, C. F., Mitchell, E. M., Mitchell, G. F., Smith, J. M. & Watson, D. G. (1991) *J. Chem. Inf. Comput. Sci.* **31**, 187-204.
- Besler, B. H., Merz, K. M. & Kollman, P. A. (1990) *J. Comput. Chem.* **11**, 431-439.
- Billington, D. C., Baker, R., Kulagowski, J. J. & Mawer, I. M. (1987) *J. Chem. Soc. Chem. Commun.*, 314-316.
- Kunkel, T. A., Roberts, J. D. & Zabor, R. A. (1987) *Methods Enzymol.* **154**, 367-382.
- Pollack, S. J., Knowles, M. R., Atack, J. R., Broughton, H. B., Ragan, C. I., Osborne, S. & McAllister, G. (1993) *Eur. J. Biochem.* **217**, 281-287.
- McAllister, G., Whiting, P., Hammond, E. A., Knowles, M. R., Atack, J. R., Bailey, F. J., Maigetter, R. & Ragan, C. I. (1992) *Biochem. J.* **284**, 749-752.
- Ragan, C. I., Watling, K. J., Gee, N. S., Aspley, S., Jackson, R. G., Reid, G. G., Baker, R., Billington, D. C., Barnaby, R. J. & Leeson, P. D. (1988) *Biochem. J.* **249**, 143-148.
- Jackson, R. G., Gee, N. S. & Ragan, C. I. (1989) *Biochem. J.* **264**, 419-422.
- Ganzhorn, A. J. & Chanal, M.-C. (1990) *Biochemistry* **29**, 6065-6071.
- Leech, A. P., Baker, G. R., Shute, J. K., Cohen, M. A. & Gani, D. (1993) *Eur. J. Biochem.* **212**, 693-704.
- Greasley, P. J. & Gore, M. G. (1993) *FEBS Lett.* **331**, 114-118.
- Zhang, Y., Liang, J.-Y. & Lipscomb, W. N. (1993) *Biochem. Biophys. Res. Commun.* **190**, 1080-1083.
- Zhang, Y., Liang, J.-Y., Huang, S., Ke, H. & Lipscomb, W. N. (1993) *Biochemistry* **32**, 1844-1857.
- Broughton, H. B. (1994) in *Topics in Molecular Modelling and Drug Design*, ed. Vinter, J. G. (Macmillan, London), in press.
- Baker, R., Kulagowski, J. J., Billington, D. C., Leeson, P. D., Lennon, I. C. & Liverton, N. (1989) *J. Chem. Soc. Chem. Commun.*, 1383-1385.
- Baker, R., Leeson, P. D., Liverton, N. J. & Kulagowski, J. J. (1990) *J. Chem. Soc. Chem. Commun.*, 462-464.
- Knowles, J. R. (1980) *Annu. Rev. Biochem.* **49**, 877-919.
- Shute, J. K., Baker, R., Billington, D. C. & Gani, D. (1988) *J. Chem. Soc. Chem. Commun.*, 626-628.
- Baker, G. R. & Gani, D. (1991) *Bioorg. Med. Chem. Lett.* **1**, 193-196.
- Vallee, B. L. & Auld, D. S. (1993) *Acc. Chem. Res.* **26**, 543-551.
- Vincent, J. B., Crowder, M. W. & Averill, B. A. (1992) *Trends Biochem. Sci.* **17**, 105-110.
- Kim, E. E. & Wyckoff, H. W. (1991) *J. Mol. Biol.* **218**, 449-464.
- Derbyshire, V., Freemont, P. S., Sanderson, M. R., Beese, L., Friedman, J. M., Joyce, C. M. & Steitz, T. A. (1988) *Science* **240**, 199-201.
- Freemont, P. S., Friedman, J. M., Beese, L. S., Sanderson, M. R. & Steitz, T. A. (1988) *Proc. Natl. Acad. Sci. USA* **85**, 8924-8928.
- Beese, L. S. & Steitz, T. A. (1991) *EMBO J.* **10**, 25-33.
- Herschlag, D. & Jencks, W. P. (1987) *J. Am. Chem. Soc.* **109**, 4665-4674.
- Herschlag, D. & Jencks, W. P. (1990) *Biochemistry* **29**, 5172-5179.